Journal of Drug Delivery Science and Technology 57 (2020) 101688

Contents lists available at ScienceDirect

Journal of Drug Delivery Science and Technology

journal homepage: www.elsevier.com/locate/jddst

Solubilization of itraconazole by surfactants and phospholipid-surfactant mixtures: interplay of amphiphile structure, pH and electrostatic interactions

Zahari Vinarov[a,*], Gabriela Gancheva[a], Nikola Burdzhiev[b], Slavka Tcholakova[a]

[a] Department of Chemical and Pharmaceutical Engineering, Faculty of Chemistry and Pharmacy, Sofia University, 1164, Sofia, Bulgaria
[b] Department of Organic Chemistry and Pharmacognosy, Faculty of Chemistry and Pharmacy, Sofia University, 1164, Sofia, Bulgaria

ARTICLE INFO

Keywords:
Itraconazole
Poorly water-soluble drugs
Solubilization
Surfactants
Phospholipids
Electrostatic interactions

ABSTRACT

Although surfactants are frequently used in enabling formulations of poorly water-soluble drugs, the link between their structure and drug solubilization capacity is still unclear. We studied the solubilization of the "brick-dust" molecule itraconazole by 16 surfactants and 3 phospholipid:surfactant mixtures. NMR spectroscopy was used to study in more details the drug-surfactant interactions. Very high solubility of itraconazole (up to 3.6 g/L) was measured in anionic surfactant micelles at pH = 3, due to electrostatic attraction between the oppositely charged (at this pH) drug and surfactant molecules. ^{1}H NMR spectroscopy showed that itraconazole is ionized at two sites (2+ charge) at these conditions: in the phenoxy-linked piperazine nitrogen and in the dioxolane-linked triazole ring. The increase of amphiphile hydrophobic chain length had a markedly different effect, depending on the amphiphile type: the solubilization capacity of single-chain surfactants increased, whereas a decrease was observed for double-chained surfactants (phosphatidylglycerols). The excellent correlation between the chain melting temperatures of phosphatidylglycerols and itraconazole solubilization illustrated the importance of hydrophobic chain mobility. This study provides rules for selection of itraconazole solubilizers among classical single-chain surfactants and phospholipids. The basic physics underpinning the described effects suggests that these rules should be transferrable to other "brick-dust" molecules.

1. Introduction

Poor aqueous solubility of low-molecular weight lead compounds is a commonly encountered problem in drug development [1], which has been attributed to the highly lipophilic requirements of modern drug targets [2]. The low drug solubility in water is one of the two major factors that lead to low or highly variable oral bioavailability, as outlined by the Biopharmaceutics classification system (BCS) [3]. Hence, a variety of formulation approaches aimed at increasing solubility and oral bioavailability have been established [4].

The development of such enabling technologies usually includes the selection of one or several model compounds with unfavorable physicochemical properties. Itraconazole is one such compound, which displays an extremely low aqueous solubility (≈1 ng/mL for the neutral form [5]) and high permeability (BCS class II [6]). It belongs to the "brick-dust" group of molecules, which are characterized by solid-state limited solubility, due to their strong crystal lattice [7,8]. Itraconazole has a relatively high molecular weight of 705.6 g/mol and is a weak base (pKa = 2 and 4 [5]).

However, the usual approach to increase drug solubility by salt formation [9] does not provide sufficient increase in itraconazole solubility to warrant direct application in drug development [10]. Hence, the marketed product of itraconazole (Sporanox®) solves the problem by solubilizing itraconazole in a concentrated (40%) cyclodextrin solution at pH = 2 for the oral solution [11] and pH = 4.5 for parenteral application [12]. The oral solution increases significantly the bioavailability, compared to the Sporanox® solid dispersion capsule formulation [13].

Itraconazole has been widely used as a model compound for development of advanced drug formulations. Considerable attention has been devoted to amorphous solid dispersions [14–20], which aim at ensuring fast dissolution kinetics and drug supersaturation in the small intestine, hence leading to increased absorption and bioavailability [21–23]. Liposomes have also been considered as potential vehicles for

* Corresponding author. Department of Chemical and Pharmaceutical Engineering Faculty of Chemistry and Pharmacy, Sofia University, 1 James Bourchier Ave, 1164, Sofia, Bulgaria.
E-mail address: zv@lcpe.uni-sofia.bg (Z. Vinarov).

https://doi.org/10.1016/j.jddst.2020.101688
Received 12 February 2020; Received in revised form 19 March 2020; Accepted 22 March 2020
Available online 27 March 2020
1773-2247/

itraconazole delivery by combining phospholipids with polymers, such as chitosan [24], or with bile salts [25] and cholesterol [26]. Polymeric micelles [27], protein [28] and polymeric nanoparticles [29–31] have also been used as itraconazole vehicles.

Lipid-based formulations have recently reappeared on the drug delivery landscape [32,33] and have been shown to improve significantly itraconazole release [34,35], as well as oral bioavailability in rats [36]. Due to the relatively low intrinsic solubility of itraconazole in the lipid excipients used to prepare these formulations [37], lipophilic ionic liquids of itraconazole have been prepared, which are then loaded in a lipid-based drug delivery vehicle to provide enhanced itraconazole absorption and oral bioavailability [38–40].

However, many of the developed enabling technologies still face challenges that need to be overcome in order to increase their use in new drug products [41]. For example, the high degree of compositional and structural complexity, which leads to incomplete mechanistic understanding of formulation performance, stability and excipients selection criteria, impedes the direct use of such technologies in pharmaceutical GMP manufacturing conditions [42–44].

Surfactants are one of the excipients, which are frequently used in advanced formulations for delivery of poorly water-soluble drugs (e.g. lipid-based formulations, liposomes, nanoparticles). Nonetheless, the link between their molecular structure and the drug solubilization capacity is still largely unexplored. For example, although the increased solubilization capacity with increasing surfactant hydrophobic chain length has been well documented for many types of drugs [45–50], there are also reports of the opposite behavior, with no clear mechanistic explanation [51]. The surfactant hydrophilic head group can also affect dramatically drug solubility [45–49,52], and while in some cases the major drivers for solubilization have been identified as electrostatic [46] or ion-dipole interactions [45,47], there is still not enough information to allow in-depth mechanistic understanding on the molecular level.

In an effort to increase the knowledge of how surfactant structure determines the solubility enhancement of “brick-dust” pharmaceutical molecules, we studied the solubilization of itraconazole by a set of 16 surfactants. The set includes surfactants of several families with positive, negative or neutral charge of the hydrophilic head group, as well as with varying length of the hydrophobic chain. The experiments were performed at two pH values, at which the itraconazole molecule was in its neutral state (pH = 6.5) or positively charged (pH = 3). After identifying the surfactant structural features that govern drug solubilization, an attempt was made to use the same principles in designing a biocompatible, solubilized formulation of itraconazole, consisting of a mixture of appropriate surfactant and phospholipid at acidic pH. NMR spectroscopy was used to gain further insight on the state of the solubilized drug molecule.

2. Materials and methods

2.1. Materials

The relationship between drug solubilization and surfactant molecular structure was investigated by using a set of 16 surfactants. Two groups of nonionic surfactants were studied: polysorbates and alcohol ethoxylates. Of the anionic surfactants family, we studied alkylsulfates (hydrophobic chain lengths of C_{10}, C_{12} and C_{14}), ethoxylated dodecylsulfates and sodium dioctylsulfosuccinate. The cationic surfactants we studied were alkyltrimethylammonium bromides with hydrophobic chain lengths of C_{12}, C_{14} and C_{16}. Biocompatible solubilized formulations of itraconazole were explored by using 3 phosphatidylglycerol lipids with chain lengths of C_{14}, C_{16} and C_{18}. Itraconazole was obtained from TCI (purity > 98%). The abbreviations and the properties of the surfactants and phospholipids studied, as well as the molecular structure of itraconazole are summarized in Table 1, whereas the surfactant critical micellar concentration (CMC) values used for calculation of the solubilization capacity are presented in the Supporting information.

Hydrochloric acid (Sigma, 32%), citric acid (Teokom, > 99%), Na_2HPO_4 (Sigma, 99%) and KH_2PO_4 (Teokom, 99%) were used to prepare buffer solutions for the drug solubilization experiments. Mobile phase solvents for HPLC analysis include methanol (HPLC grade, Sigma, 99.9%) and glycine (Valerus, 99%) solution in water. All aqueous solutions and phases were prepared using deionized water from water-purification system Elix 3 (Millipore, USA).

2.2. Itraconazole solubility in buffered surfactant solutions

Excess amount of drug was weighed in a 20 mL glass bottle and 10 mL buffered surfactant solution was added. The buffers used were 40 mM Na_2HPO_4 + 80 mM citric acid (pH = 3) and 63 mM Na_2HPO_4 + 121 mM KH_2PO_4 (pH = 6.5). The mixture was stirred with a magnetic stir bar at 400 rpm for 24 h at 37 °C. Constant surfactant concentration which was much higher than the CMC of all studied surfactants was used (C_S = 60 mM). After incubation, the itraconazole suspension was filtered through 0.2 μm NYLON syringe filter to eliminate all undissolved particles.

After separation of the undissolved particles, the concentration of dissolved drug in the obtained clear aqueous solutions was determined by HPLC-UV. Every step of the procedure was carried out at T = 37 °C.

2.3. Itraconazole solubility in phospholipid-surfactant mixtures

Itraconazole solubilization in the colloidal aggregates formed by mixtures of AOT and phosphatidylglycerol phospholipids with varying hydrophobic chain length, was studied by using the following procedure. First, a solution of AOT was prepared, by dissolving an appropriate amount of the surfactant in 3 mL buffer solution (pH = 3 or 2.5), in a 5 mL glass bottle. pH was kept constant by using citrate buffer composed of 41 mM citric acid and 9 mM sodium citrate, adjusted with citric acid. Then, the appropriate amount of phospholipid was added and the obtained suspension was sonicated for 60 s by using a 3 mm diameter sonotrode, set at power output of 250 W (SKL-650 W sonicator, Syclon). The amounts of AOT and phospholipid weighed corresponded to a total amphiphile concentration of 40 mM and a ratio of 1:1. Afterwards, excess itraconazole powder was added and the mixture was stirred for 24 h and T = 37 °C. After incubation, the itraconazole suspension was filtered through 0.2 μm NYLON syringe filter to eliminate all undissolved particles. The concentration of dissolved drug in the obtained aqueous solutions was determined by HPLC-UV.

2.4. HPLC-UV analysis

HPLC analysis was carried out on a Shimadzu apparatus, equipped with two high-pressure mixing binary gradient pumps (LC-20AD), autosampler (SIL-10ADvp), four-line membrane degasser (DGU-14A), wide temperature range column oven (CTO-10ASvp) and a dual-wave length UV-VIS detector (SPD-10Avp). We used an Ascentis C18 column (250 mm × 4.6 mm, 5 μm particle size) and methanol:glycine buffer (85:15) mobile phase. The glycine buffer was prepared in water at a concentration of 40 mM and pH = 8. Isocratic elution for 10 min with total flow of 1 mL/min and injection volume of 20 μL was used. UV detection was performed at λ = 205 nm. Column temperature was set at 40 °C. The retention time of itraconazole was t_r = 7.2 min. The concentration of solubilized drug was determined by using a standard curve (R^2 = 0.999), which was prepared by dissolving a known amount of drug in a mixture of methanol and 0.1 M HCl at a ratio of 1:1.

2.5. Solubilization capacity calculation

To compare the itraconazole solubilization efficiency of the different surfactants we used the molar solubilization capacity, defined as follows [53]:

Table 1
Properties of the drug and amphiphiles studied.

Name	Acronym used in text	Supplier, purity	Molecular mass, g/mol	Structure
Itraconazole	–	TCI, 98%	706	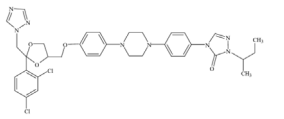
Sodium decyl sulfate	$C_{10}SO_4Na$	Merck, 99%	260	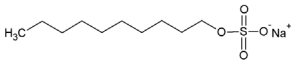
Sodium lauryl sulfate	$C_{12}SO_4Na$	Arcos, 99%	288	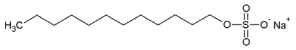
Sodium tetradecyl sulfate	$C_{14}SO_4Na$	Merck, 95%	316	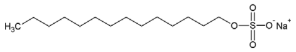
Sodium lauryl ethoxy (1) sulfate	$C_{12}E_1SO_4Na$	Stepan Co., 70%	332	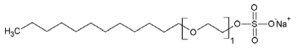
Sodium lauryl ethoxy (3) sulfate	$C_{12}E_3SO_4Na$	Stepan Co., 70%	420	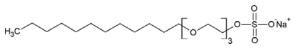
Sodium dioctyl-sulfosuccinate	AOT	Sigma	445	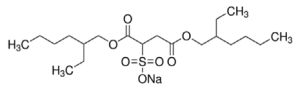
Sodium taurodeoxy-cholate	STDC	Sigma, 97%	522	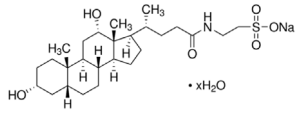
Tween 20	T20	Sigma – Aldrich	1228	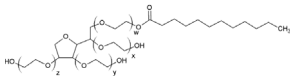
Tween 60	T60	Sigma – Aldrich	1309	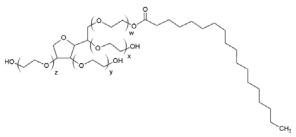
Tween 80	T80	Sigma – Aldrich	1310	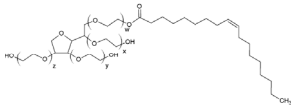
Polyoxyethylene (23) lauryl ether	$C_{12}E_{23}$	Sigma – Aldrich	1198	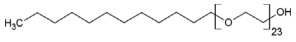
Polyoxyethylene (20) cetyl ether	$C_{16}E_{20}$	Sigma	1124	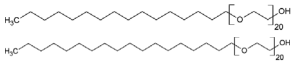
Polyoxyethylene (20) stearyl ether	$C_{18}E_{20}$	Sigma	1152	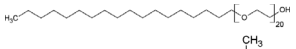
Dodecyl trimethyl ammonium bromide	$C_{12}TAB$	Sigma – Aldrich, 98%	308	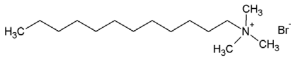
Tetradecyl trimethyl ammonium bromide	$C_{14}TAB$	Sigma, 99%	336	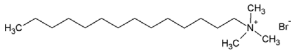
Cetyltrimethyl ammonium bromide	$C_{16}TAB$	Merck, 99%	364	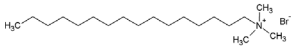
Sodium dimyristoyl phosphatidyl glycerol	DMPG	NOF, 99%	698	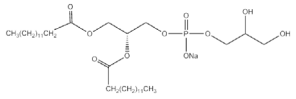
Sodium dipalmitoyl phosphatidyl glycerol	DPPG	NOF, 99%	745	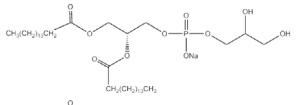
Sodium distearoyl phosphatidyl glycerol	DSPG	NOF, 99%	801	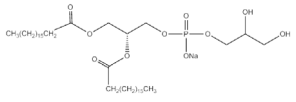

$$\chi = \left(\frac{S_{tot} - S_W}{C_S - CMC}\right) \times 1000 \quad (1)$$

where S_{tot} is the measured apparent molar drug solubility in presence of surfactants, S_W is the solubility of the drug at the respective pH, C_S is the molar surfactant concentration and CMC is the critical micelle concentration of the respective surfactant. Thus, the solubilization capacity accounts for the different CMC of the surfactants and considers only the drug and surfactant molecules that are present in the micellar aggregates (without the contribution of surfactant monomers and the drug molecules dissolved in buffer solution). The CMC values of the surfactants studied are presented in the Supporting information. As itraconazole solubility in the buffers used (pH = 3 and 6.5) was too low to measure, the values used for the solubility were 1 ng/mL (for the

neutral form, pH = 6.5) and 1 μg/mL (pH ≈ 1) [5].

2.6. ^{1}H NMR study of itraconazole ionization

NMR spectra were obtained on a Bruker Avance III HD 500 MHz spectrometer (Rheinstetten, Germany). A Bruker broadband high-resolution probe (Observe) fitted with an actively shielded single axis Z-gradient was used. Experiments were conducted at T = 37 °C. The studied samples were prepared as described in section 2.2, except that deuterium oxide (99.8 atom % D) was used instead of water to dissolve the buffer and the surfactants. TMSP-Na-2,2,3,3-d4 was added to the sample as internal standard (0 ppm) prior to measurement. The resolution of the obtained spectra is 0.001 ppm and the standard error in the determination of the chemical shifts is < 0.002 ppm. Topspin 3.5 pl6 software package (Bruker) was used for spectrum collection and data analysis.

3. Experimental results

3.1. Effect of pH on itraconazole solubility in surfactant solutions

The solubility of itraconazole as a function of surfactant type at pH = 3 and 6.5 is presented in Fig. 1. At acidic conditions (pH = 3), the solubility of itraconazole increased dramatically in all anionic surfactant solutions, reaching a maximum of 3.6 g/L in the solution of the $C_{14}SO_4Na$ alkylsulfate surfactant. Increase of pH to the near-neutral value of 6.5 decreased very strongly the solubility of itraconazole in anionic surfactant solutions: for example, a decrease of more than one order of magnitude, from 1.9 (pH = 3) to 0.1 g/L (pH = 6.5) was determined for the $C_{12}SO_4Na$ surfactant.

In contrast, the effects of pH on the other studied surfactant types were much smaller: for the nonionic surfactants, the solubility of itraconazole increased slightly at pH = 3 (range of 0.02–0.06 g/L), compared to pH = 6.5 (0.01–0.03 g/L). For the cationic surfactants, there was either no effect (C_{12}TAB, C_{14}TAB), or a very slight decrease (C_{16}TAB) in the solubility. However, it is clearly seen that the solubility of itraconazole in solutions of anionic surfactants at pH = 6.5 and for the cationic and nonionic surfactants at both studied pHs (solubility range of 0.003–0.11 g/L) was much lower, compared to the anionic surfactants at pH = 3.

One can note that there are considerable differences (orders of magnitude) in the solubility of itraconazole for surfactants with the same charge, or even within the same surfactant family: 0.35 g/L for $C_{10}SO_4Na$, compared to 3.6 g/L for $C_{14}SO_4Na$, both at pH = 3. These effects of surfactant structure are studied in the next section.

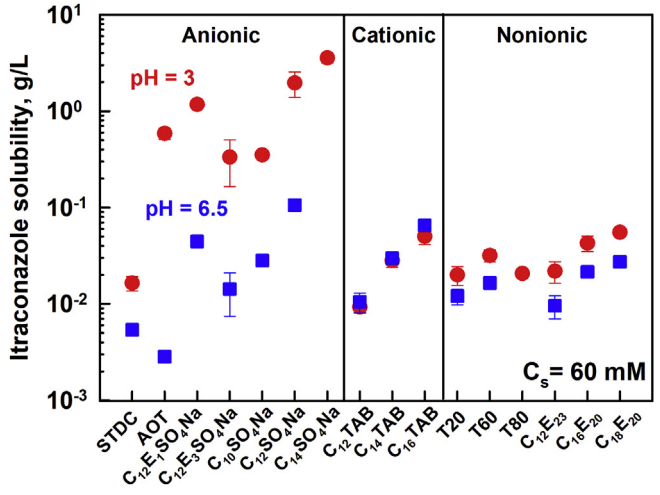

Fig. 1. Itraconazole solubility in 60 mM surfactant solutions at pH = 3 (red circles) and 6.5 (blue squares), n = 3–9. Data for $C_{14}SO_4Na$ at pH = 6.5 is not shown, due to insufficient solubility of the surfactant at these conditions. The error bars can be smaller than the symbols. (For interpretation of the references to colour in this figure legend, the reader is referred to the Web version of this article).

3.2. Effect of surfactant molecular structure on itraconazole solubilization

To clarify the effects of the main structural characteristics of a surfactant molecule on itraconazole solubility, it is important to compare the results of the individual surfactants in an appropriate framework. The molar solubilization capacity (as defined in section 2.5), provides such a format of comparison, as it accounts for the CMC of each individual surfactant, as well as for the solubility of the drug in buffer solutions.

Even when using the molar solubilization capacity, however, the effects of the hydrophobic chain and hydrophilic headgroup might be confounded if both are varied simultaneously. To resolve this issue, we study the effect of each parameter separately: *viz.* The effect of the hydrophobic chain is studied for surfactants with an identical hydrophilic head group, and vice-versa. We first present the effect of the hydrophilic headgroup, which appears to govern the solubilization capacity, followed by the effect of the hydrophobic chain.

3.2.1. Surfactant hydrophilic head group

The effect of the type hydrophilic headgroup was studied in surfactants with a constant hydrophobic chain length of 12 carbon atoms, as they presented the widest variety of head group types from the surfactants used in the current study, see Fig. 2. One can see the very strong effect of pH for all negatively charged head groups, which results in much higher solubilization capacity (8–47 mM/M) of these surfactant micelles at pH = 3, in accordance with the results presented in section 3.1. The nonionic headgroups which are comprised of an ethoxy chain (for the ethoxylated dodecanol, $C_{12}EO_{23}$) and an ethoxylated sorbitan ring (for the polysorbate 20 surfactant) show orders of magnitude lower solubilization capacity (0.5 and 0.4 mM/M, respectively). Lowest solubilization capacity was calculated for the positively charged TAB micelles (0.2 mM/M).

At pH = 6.5, highest solubilization capacity was again determined for the sulfate head group, followed by the ethoxylated (1) sulfate headgroup. No significant difference was observed between the solubilization capacities of the negatively charged ethoxy (3) sulfate, the positively charged TAB and the two nonionic head groups. Common

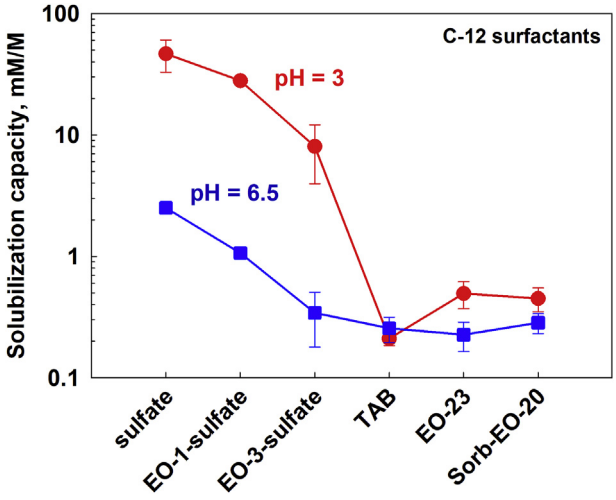

Fig. 2. Micellar solubilization capacity for itraconazole of dodecyl surfactants with different hydrophilic head groups at pH = 3 (red circles) and 6.5 (blue circles). The error bars can be smaller than the symbols. (For interpretation of the references to colour in this figure legend, the reader is referred to the Web version of this article).

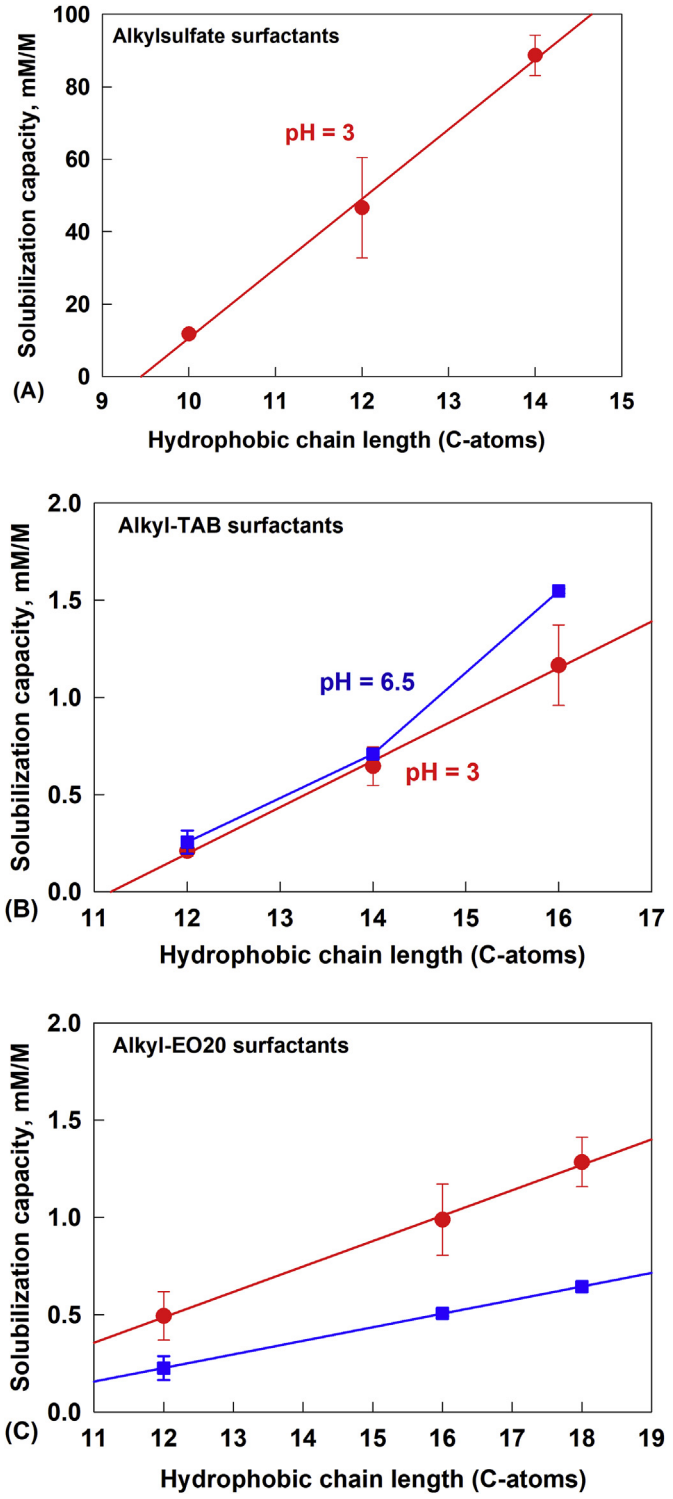

Fig. 3. Micellar solubilization capacity for itraconazole of (A) alkylsulfate, (B) alkyl-trimethyammonium bromide and (C) ethoxylated (20-23) alcohol surfactants at pH = 3 (red circles) and 6.5 (blue squares). The error bars can be smaller than the symbols. (For interpretation of the references to colour in this figure legend, the reader is referred to the Web version of this article).

phenomena observed at both pH were the gradual decrease of the solubilization capacity of the sulfate head group upon its ethoxylation and the identical solubilization capacity of the ethoxy- and sorbitan-ethoxy (polysorbate) headgroups.

3.2.2. Surfactant hydrophobic chain length

The effect of surfactant hydrophobic chain length on the solubilization capacity for itraconazole was determined separately for each homologue series of surfactants. Hence, the number of carbon atoms in the hydrophobic chain was varied, while keeping the same hydrophilic head group, see Fig. 3.

For all studied surfactant types, the solubilization capacity increased linearly with the increased hydrophobic chain length, at both studied pH values. Due to the very strong effect of pH on the solubilization capacity of the negatively charged alkylsulfate surfactants, the data for pH = 3 and 6.5 lie on completely different scales, which prevents their direct visual comparison. For the nonionic surfactants, the solubilization capacity at pH = 3 is shifted slightly above pH = 6.5. This different intercept is in accordance with the slightly higher solubilization capacity of itraconazole, observed for nonionic surfactant at low pH. Such shift is not observed for the positively charged TAB surfactants.

3.3. Solubilization in phospholipid:surfactant mixtures

The results presented in the previous sections showed that a considerable increase of itraconazole solubility is obtained via solubilization in negatively charged surfactant micelles at acidic pH. To check if similar results can be obtained with surfactants with better biocompatibility, experiments were performed with mixtures of the surfactant AOT (sodium docusate) and different phospholipids. This surfactant was chosen due to the following reasons: (1) it has low toxicity (it is allowed for use in parenteral preparations [54]), (2) it is negatively charged and (3) it has been shown to form aggregates with very high drug solubilization capacity when combined with phospholipids [46]. Negatively charged phospholipids of the phosphatidylglycerol type with different hydrophobic chain length were mixed with AOT at a ratio of 1:1, which was previously shown to provide high solubilization capacity for albendazole [46].

The obtained results are presented in Fig. 4. At pH = 3, highest itraconazole solubility of 0.13 g/L was measured for the phospholipid with the shortest chain length (2 × C14, DMPG). Solubility decreased significantly with the increase of the hydrophobic chain length of the phospholipid: 0.06 g/L for 2 × C16, DPPG and 0.03 g/L for 2 × C18, DSPG. Although the measured solubilities are orders of magnitude higher, compared to the solubility of itraconazole at acidic conditions (0.001 g/L at pH = 1 [5]), they are significantly lower than the ones

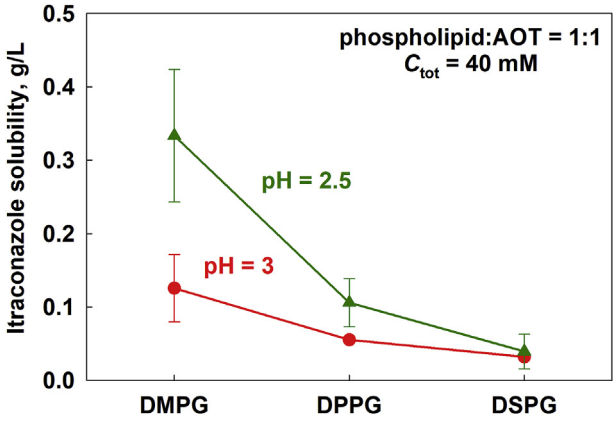

Fig. 4. Itraconazole solubility in mixtures of sodium docusate (AOT) with phosphatidyl-glycerol phospholipids with two C-14 (DMPG), C-16 (DPPG) or C-18 (DSPG) hydrophobic chains at pH = 3 (red circles) or 2.5 (green triangles). The surfactant-to-phospholipid ratio is constant at 1:1 and the total surfactant + phospholipid concentration is 40 mM. (For interpretation of the references to colour in this figure legend, the reader is referred to the Web version of this article).

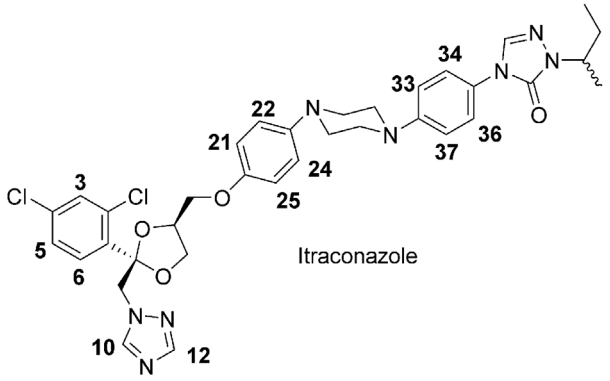

Fig. 5. Numbering of the aromatic H atoms in itraconazole (corresponds to Ref. [55]).

measured for the alkylsulfate surfactants. To check if the solubility in the biocompatible AOT:phospholipid mixtures can be further improved, additional experiments at lower pH = 2.5 were performed. Indeed, the solubility of itraconazole was improved strongly at these conditions, reaching ca. 0.33 g/L for DMPG:AOT. The trend of decreasing solubility with increasing phospholipid chain length remained the same.

3.4. ^{1}H NMR study of itraconazole solubilized in micelles

To gain more insight on the molecular interactions entailing itraconazole (Fig. 5) solubilization in anionic surfactant micelles at acidic conditions (pH = 3), we used ^{1}H NMR spectroscopy. Spectrum of itraconazole solubilized in $C_{12}SO_4Na$ micelles at pH = 3 was taken (see Fig. 1 in the Supporting information). The chemical shifts of itraconazole can be divided in three groups, according to Inkmann and Holzgrabe [55]. The first group is between 0.5 and 2 ppm and corresponds to the H signals of the aliphatic part of the molecule. The second range from 3.5 to 5.1 ppm consists of all signals belonging to CH_2 groups connected to N or O. However, both of these ranges coincide with the ranges of the $C_{12}SO_4Na$ signals, which renders the complete description of the signals impossible. Fortunately, the third region of itraconazole signals originate from its aromatic rings, which do not overlap with any of the $C_{12}SO_4Na$ signals. This part of the spectrum is presented in Fig. 6.

The chemical shifts of ^{1}H in the aromatic range of the solubilized itraconazole molecule are described in Table 2, alongside with the data for protonated itraconazole from the study of Inkmann and Holzgrabe [55]. The signals for the protons in the dichlorophenyl moiety (H-3, 5 and 6), which are not connected with the protonation sites, perfectly replicate the results obtained by Inkmann and Holzgrabe, despite some differences between the two studies (e.g. solvent type, spectra acquisition conditions). The rest of the signals also match very well, especially H-10, 12 and H-22:24, which are the protons that are most affected by the protonation.

4. Discussion

Most of the experiments in the study were performed at pH 3 and 6.5. These pH values were chosen by considering the physicochemical properties of itraconazole (e.g. its pKa of 4 and 2 [5]), the acceptable pH range in drug formulation development and the conditions the drug can encounter after administration. The acidic pH of 3 ensures protonation of the itraconazole molecule and allows evaluation of the electrostatic interactions between the positively charged drug and the ionic surfactant micelles. At the same time, pH = 3 is relevant also in the formulation development context: it is in the acceptable range for parenterally administered formulations [56], while it also provides valuable information for the behavior of itraconazole at stomach conditions in pediatric populations [57]. On the other hand, the itraconazole molecule is uncharged at pH = 6.5, which is also the pH characteristic for the human small intestine [58].

The results presented in Fig. 1 showed that pH has a dramatic effect on itraconazole solubilization by anionic surfactants: itraconazole solubility of up to 3.6 g/L was measured at pH = 3, whereas the maximum solubility at pH = 6.5 was ca. 0.1 g/L. The solubilization of 3.6 g/L itraconazole was obtained by using 60 mM $C_{14}SO_4Na$ (corresponding to 1.9 wt %). The latter is superior to β-cyclodextrin (used in the marketed itraconazole formulation, Sporanox), which provides a seven-fold lower itraconazole solubilization (≈0.5 g/L) for the same weight concentration of excipient [11,12]. Other approaches for itraconazole solubilization in aqueous media have achieved a maximum of ≈0.3 g/L (solid dispersions, pH = 1 [15]) and 15 g/L (polymeric micelles, excipient concentration of 9 wt % [27]).

Such significant effect of pH, as the one observed in the current study, is usually explained by a change in the ionization state of at least one of the considered molecules. The sulfate group, which brings the negative charge of the alkylsulfate surfactants, has a pKa close to 0 [59]: hence, it is not affected by switching the pH from 6.5 to 3.

However, the situation is different for itraconazole, which has pKa of 4 and 2 [5]: the drug molecule changes its state from unionized at pH = 6.5 to positively charged at pH = 3. The ^{1}H NMR spectroscopy measurements performed in the current study matched very well the work of Inkmann and Holzgrabe, who showed that such a spectrum corresponds to an itraconazole molecule protonated at 2 positions: in the triazole ring, linked to the dioxolane moiety of the molecule and at the piperazine nitrogen, connected to the phenoxy substituent. The latter indicates that itraconazole solubilized in anionic surfactant micelles at pH = 3 has a charge of 2+.

Since the big increase of itraconazole solubility at pH = 3 was observed in solutions of all studied negatively charged surfactants, we can suggest that the effect is due to electrostatic interactions. This hypothesis is confirmed by the fact that the solubility of itraconazole at pH = 3 decreases slightly for the positively charged C_nTAB surfactants, compared to pH = 6.5. The latter observation fits well with the electrostatic interaction hypothesis: the repulsion between the similarly charged (at pH = 3) drug and surfactant molecules leads to the decreased solubility. Therefore, we can conclude that the high solubility of itraconazole in solutions of anionic surfactants at pH = 3 is due to electrostatic attraction between the oppositely charged (at this pH) drug and surfactant molecules in the micelles. The interaction is enhanced by the 2+ charge of itraconazole at these conditions. The combination of appropriate surfactant and pH, leading to significant increase in drug solubility due to electrostatic attraction was observed also for other poorly water-soluble drugs, such as albendazole [46] and ibuprofen [60,61].

Further analysis of the data showed an additional, pH independent effect of the surfactant hydrophilic head groups on itraconazole solubilization. At both studied pH, the sulfate head group has significantly higher solubilization capacity, compared to all other head groups studied. Although the same effect has been observed also for the weak base albendazole [46] and for neutral drugs, such as progesterone [47], fenofibrate and danazol [45], the unifying mechanism is still unclear. One possible explanation is that the smaller size of the sulfate head group facilitates the packing of the drug and surfactant molecules in the micelles, viz. a steric effect. Such explanation has already been proposed to explain the significant decrease of the solubilization capacity when ethylene oxide units are added between the lauroyl chain and the sulfate head group for other drugs [45–47]. Another possibility is that ion-dipole interactions contribute to the solubilization capacity, as has been shown for progesterone [47] and danazol [45]. Molecular dynamics simulations might provide further insight on the mechanism of this interesting effect, however, such efforts have not been undertaken yet, due to the significant computational resources required to model solubilization in micellar systems that include multiple surfactant and drug pairs.

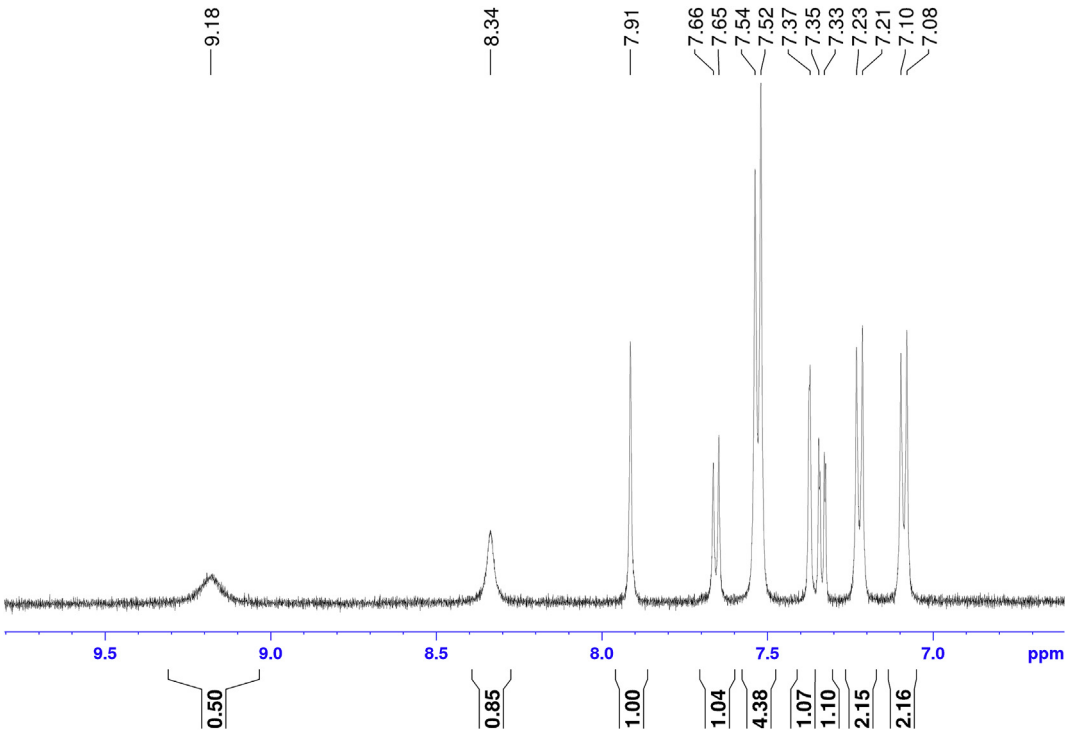

Fig. 6. Aromatic region of the ^{1}H NMR spectrum of itraconazole, solubilized in $C_{12}SO_4Na$ micelles at pH = 3.

By calculating the surfactant solubilization capacity and accounting for the micellar aggregation number (N_{agg}), we can estimate the number of drug molecules per micelle (see Table 3). Although the literature values used for N_{agg} are obtained at slightly different conditions than the ones in the current study, the estimated number of drug molecules per micelle provides a useful illustration of the degree of drug solubilization. As N_{agg} varies in a relatively small range for the studied set of surfactants (N_{agg} = 40 to 150), the average number of drug molecules per micelle correlates well with the measured drug solubility and the calculated solubilization capacity. Hence, the maximal number of itraconazole molecules per micelle (around 6) is obtained for $C_{14}SO_4Na$ at pH = 3. The number of itraconazole molecules per micelle for anionic surfactants at pH = 6.5, as well as for cationic and nonionic surfactants at both pH studied is much less than 1. For these systems, 1 itraconazole molecule is solubilized per 5 to 100 micelles, illustrating their very low solubilization capacity.

The increase of itraconazole solubilization capacity for single-chain surfactants with longer hydrophobic chain length (Fig. 3) is a commonly observed effect that has been reported for many other drugs [45–50]. The latter is believed to be caused by the increased space available for solubilization of drugs in the micelles, due to the increased volume of the hydrophobic core and of the palisade layer in micelles formed by longer chain length surfactants.

Table 3
Surfactant aggregation number, itraconazole solubilization capacity and number of itraconazole molecules solubilized per 1 micelle.

Surfactant	Nagg	Sol. cap., mM/M		Itraconazole molecules per micelle	
		pH = 3	pH = 6.5	pH = 3	pH = 6.5
AOT	150 [62]	13.88	0.07	2.08	0.01
$C_{10}SO_4Na$	50 [63]	11.83	0.75	0.59	0.04
$C_{12}SO_4Na$	65 [64]	46.63	2.51	3.03	0.16
$C_{14}SO_4Na$	67 [65]	88.70	–	5.94	–
$C_{12}E_1SO_4Na$	79 [64]	27.98	1.06	2.21	0.08
$C_{12}E_3SO_4Na$	54 [64]	8.04	0.34	0.43	0.02
$C_{12}TAB$	59 [63]	0.21	0.26	0.01	0.02
$C_{14}TAB$	88 [63]	0.65	0.71	0.06	0.06
$C_{16}TAB$	135 [64]	1.17	1.55	0.16	0.21
$C_{12}E_{23}$	40 [63]	0.49	0.23	0.02	0.01
$C_{16}E_{20}$	70 [63]	0.99	0.51	0.07	0.04
$C_{18}E_{20}$	-	1.29	0.64	–	–
T20	79 [66]	0.45	0.28	0.04	0.02
T60	112 [63]	0.73	0.39	0.08	0.04
T80	133 [67]	0.47	–	0.06	–
MIN	40	0.21	0.07	0.01	0.01
MAX	150	88.70	2.51	5.94	0.21

Table 2
Chemical shifts and J-constants of aromatic ^{1}H atoms of solubilized itraconazole measured in this study, compared with the data for ionized itraconazole in mixed organic solvents + water media, obtained by Inkmann and Holzgrabe [55].

Atom number	Itraconazole solubilized in micelles, pH = 3	Itraconazole in CDCl3:CH3OD:D2O (16:8:1), after addition of 2 eq. DCl [55]
H-21:25	7.09 (d, 2H, *J* = 9.0 Hz)	7.00
H-33:37	7.22 (d, 2H, *J* = 9.0 Hz)	7.16
H-5	7.34 (dd, 1H, J = 1.9; 8.5 Hz)	7.32
H-3	7.37 (s, 1H)	7.48
H-22:24/34:36	7.53 (d, 4H, *J* = 8.7 Hz)	7.76/7.47
H-6	7.65 (d, 1H, *J* = 8.5 Hz)	7.64
H-42	7.91 (s, 1H)	7.86
H-12	8.34 (br.s. 0.7H)	8.33
H-10	9.18 (br.s. 0.5H)	9.20

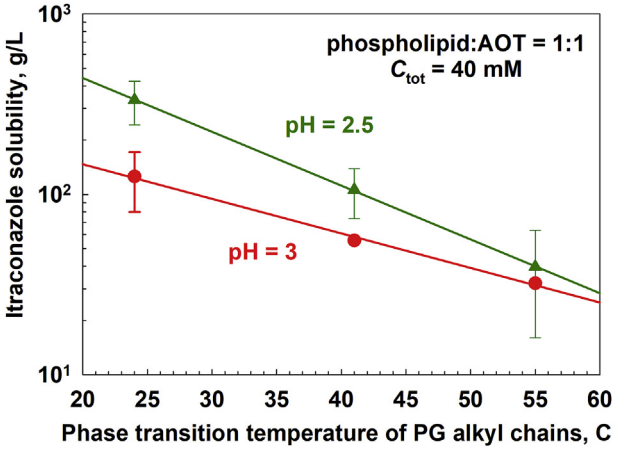

Fig. 7. Itraconazole solubility in phospholipid-AOT mixtures, as a function of the phospholipid chain melting temperature at pH = 3 (red circles) and 2.5 (green triangles). (For interpretation of the references to colour in this figure legend, the reader is referred to the Web version of this article).

However, the opposite trend was observed for the phospholipid-surfactant mixtures (Fig. 4): the solubilization of itraconazole decreased significantly with increasing the length of the phospholipid hydrophobic chains. The qualitative difference in the behavior of the pure surfactant systems and the phospholipid:surfactant mixtures could be explained if we consider the colloidal species involved in the two cases: micelles for the surfactant-only systems and vesicles for the phospholipid-AOT mixtures. Note that AOT is known to form vesicles on its own [68], as is also characteristic for the phospholipids [69] and phospholipid-AOT mixtures [46]. While the hydrophobic chains in classical surfactant micellar systems enjoy significant mobility, similar to the one in the bulk of liquid hydrocarbons [70], this is not true in the case of bilayer vesicular structures formed by phospholipids. The mobility of the alkyl chains in phospholipid bilayers is characterized by a melting (phase transition, T_c) temperature, which depends on the chain length [71]. Indeed, if the logarithm of itraconazole solubility in phospholipid-AOT mixtures is plotted as a function of the phospholipid chain melting temperature, an excellent linear relationship is obtained, see Fig. 7.

One sees that drug solubility is highest for the DMPG aggregates (T_c = 24 °C), in which the alkyl chains are in liquid state at T = 37 °C. In contrast, the alkyl chains of DPPG (T_c = 41 °C) and DSPG (T_c = 55 °C) are both in a solid-like state (viz. decreased mobility) and the measured solubility was much lower. We can therefore conclude that the solubilization of itraconazole in phosphatidylglycerol aggregates is governed by the degree of chain mobility: the looser packing of shorter chain length phospholipids facilitates the incorporation of more drug molecules in the aggregates and leads to higher drug solubilization. Furthermore, the phase transition temperature of the phospholipid chains can be used to assess drug solubility, instead of the hydrophobic chain mobility of the phospholipids, which is a difficult parameter to quantify. Phase transition temperatures of different phospholipid types and chain lengths are available in various literature sources, e.g. Ref. [71].

5. Conclusions

The solubilization of itraconazole in the colloidal aggregates of 16 surfactants and 3 phospholipid:surfactant mixtures was studied. The experiments with the surfactants were performed at pH = 3 and 6.5, where the itraconazole molecule is positively charged or neutral, respectively. The solubilization in phospholipid:surfactant mixtures was studied at pH = 2.5 and 3. NMR spectroscopy was used to gain further insight on the mechanism of itraconazole solubilization in anionic surfactant micelles at pH = 3. The main conclusions from the study can be summarized as follows:

- ✓ Very high solubility of itraconazole (up to 3.6 g/L) was achieved by solubilization in anionic surfactant micelles at pH = 3. The high solubilization is due to electrostatic attraction between the oppositely charged (at this pH) drug and surfactant molecules
- ✓ The strong interactions are due to the charge of itraconazole, which is most likely 2+ at these conditions (^{1}H NMR data). The ionization sites were identified as the phenoxy-linked piperazine nitrogen and the dioxolane-linked triazole ring
- ✓ The effect of the amphiphile hydrophobic chain length on itraconazole solubilization depends on the amphiphile type: for single-chain, micelle-forming surfactants, drug solubilization increases with the increase of surfactant chain length; in contrast, the opposite was observed for double-chained, vesicle-forming surfactants, such as the phospholipids of phosphatidylglycerol type
- ✓ Hydrophobic chain mobility is a major determinant of itraconazole solubilization in AOT:phosphatidylglycerol mixtures, as demonstrated by the excellent correlation between the chain melting temperatures of phosphatidylglycerols and itraconazole solubility

The results in the presented study provide a mechanism-based guidance for selection of itraconazole solubilizers among classical single-chain surfactants and phospholipids. The role of pH as a critical parameter governing itraconazole solubilization in anionic surfactants solutions was rationalized by considering itraconazole ionization behavior and electrostatic drug-surfactant interactions. The basic physics underpinning the described effects suggests that the obtained solubilizer selection rules could be transferrable to other drugs which share similar physicochemical properties with itraconazole (e.g. posaconazole, ketoconazole and other triazole antimycotics).

CRediT authorship contribution statement

Zahari Vinarov: Conceptualization, Methodology, Supervision, Writing - original draft, Writing - review & editing, Funding acquisition. **Gabriela Gancheva:** Investigation. **Nikola Burdzhiev:** Methodology, Investigation. **Slavka Tcholakova:** Conceptualization, Methodology, Supervision, Writing - review & editing, Funding acquisition, Project administration.

Declaration of competing interest

The authors declare that they have no known competing financial interests or personal relationships that could have appeared to influence the work reported in this paper.

Acknowledgements

The authors thank Petra Dobreva and Betina Angelska for their assistance with several drug solubilization measurements and Fatmegyul Mustan for few of the chemical structure drawings. The financial support of Bulgarian Science Fund project № DCOST 01/12 is gratefully acknowledged. This article is partly based upon work carried out under COST Action 16205 UNGAP, supported by COST (European Cooperation in Science and Technology).

Appendix A. Supplementary data

Supplementary data to this article can be found online at https://doi.org/10.1016/j.jddst.2020.101688.

References

[1] L.Z. Benet, F. Broccatelli, T.I. Oprea, BDDCS applied to over 900 drugs, AAPS J. 13 (2011) 519–547, https://doi.org/10.1208/s12248-011-9290-9.

[2] G.M. Keserü, G.M. Makara, The influence of lead discovery strategies on the properties of drug candidates, Nat. Rev. Drug Discov. (2009), https://doi.org/10.1038/nrd2796.

[3] G.L. Amidon, H. Lennernäs, V.P. Shah, J.R. Crison, A theoretical basis for a biopharmaceutic drug classification: the correlation of in vitro drug product dissolution and in vivo bioavailability, Pharm. Res. An Off. J. Am. Assoc. Pharm. Sci. (1995), https://doi.org/10.1023/A:1016212804288.

[4] B.J. Boyd, C.A.S. Bergström, Z. Vinarov, M. Kuentz, J. Brouwers, P. Augustijns, M. Brandl, A. Bernkop-Schnürch, N. Shrestha, V. Préat, A. Müllertz, A. Bauer-Brandl, V. Jannin, Successful oral delivery of poorly water-soluble drugs both depends on the intraluminal behavior of drugs and of appropriate advanced drug delivery systems, Eur. J. Pharmaceut. Sci. 137 (2019), https://doi.org/10.1016/j.ejps.2019.104967.

[5] J. Peeters, P. Neeskens, J.P. Tollenaere, P. Van Remoortere, M.E. Brewster, Characterization of the interaction of 2-hydroxypropyl-β-cyclodextrin with itraconazole at pH 2, 4, and 7, J. Pharmacol. Sci. 91 (2002) 1414–1422, https://doi.org/10.1002/jps.10126.

[6] T. Takagi, C. Ramachandran, M. Bermejo, S. Yamashita, L.X. Yu, G.L. Amidon, A provisional biopharmaceutical classification of the top 200 oral drug products in the United States, Great Britain, Spain, and Japan, Mol. Pharm. (2006), https://doi.org/10.1021/mp0600182.

[7] C.M. Wassvik, A.G. Holmén, R. Draheim, P. Artursson, C.A.S. Bergström, Molecular characteristics for solid-state limited solubility, J. Med. Chem. 51 (2008) 3035–3039, https://doi.org/10.1021/jm701587d.

[8] C.A.S. Bergström, C.M. Wassvik, K. Johansson, I. Hubatsch, Poorly soluble marketed drugs display solvation limited solubility, J. Med. Chem. 50 (2007) 5858–5862, https://doi.org/10.1021/jm0706416.

[9] A.T.M. Serajuddin, Salt formation to improve drug solubility, Adv. Drug Deliv. Rev. (2007), https://doi.org/10.1016/j.addr.2007.05.010.

[10] H. Bagavatula, S. Lankalapalli, V.S. Vinai, K. Tenneti, N. Malleswara, R. Beeraka, B.T. Bulusu, Comparative studies on solubility and dissolution enhancement of different itraconazole salts and their complexes, Adv. Pharmacol. Pharm. 2 (2014) 85–95, https://doi.org/10.13189/app.2014.020601.

[11] Sporanox Oral Solution FDA, (n.d.) 1–37.

[12] Sporanox Injection Solution FDA, (n.d).

[13] L. Willems, R. Van Der Geest, K. De Beule, Itraconazole oral solution and intravenous formulations: a review of pharmacokinetics and pharmacodynamics, J. Clin. Pharm. Therapeut. (2001), https://doi.org/10.1046/j.1365-2710.2001.00338.x.

[14] D.A. Miller, J.T. McConville, W. Yang, R.O. Williams, J.W. McGinity, Hot-melt extrusion for enhanced delivery of drug particles, J. Pharmacol. Sci. (2007), https://doi.org/10.1002/jps.20806.

[15] J.Y. Jung, S.D. Yoo, S.H. Lee, K.H. Kim, D.S. Yoon, K.H. Lee, Enhanced solubility and dissolution rate of itraconazole by a solid dispersion technique, Int. J. Pharm. 187 (1999) 209–218, https://doi.org/10.1016/S0378-5173(99)00191-X.

[16] K. Six, T. Daems, J. de Hoon, A. Van Hecken, M. Depre, M.-P. Bouche, P. Prinsen, G. Verreck, J. Peeters, M.E. Brewster, G. Van den Mooter, Clinical study of solid dispersions of itraconazole prepared by hot-stage extrusion, Eur. J. Pharmaceut. Sci. 24 (2005) 179–186, https://doi.org/10.1016/J.EJPS.2004.10.005.

[17] Y. Zhong, G. Jing, B. Tian, H. Huang, Y. Zhang, J. Gou, X. Tang, H. He, Y. Wang, Supersaturation induced by Itraconazole/Soluplus® micelles provided high GI absorption in vivo, Asian J. Pharm. Sci. 11 (2016) 255–264, https://doi.org/10.1016/j.ajps.2015.07.001.

[18] K. Zhang, H. Yu, Q. Luo, S. Yang, X. Lin, Y. Zhang, B. Tian, X. Tang, Increased dissolution and oral absorption of itraconazole/Soluplus extrudate compared with itraconazole nanosuspension, Eur. J. Pharm. Biopharm. (2013), https://doi.org/10.1016/j.ejpb.2013.03.002.

[19] Y.J. Park, J.J. Xuan, D.H. Oh, P. Balakrishnan, H.J. Yang, W.H. Yeo, M.K. Lee, H.G. Choi, C.S. Yong, Development of novel itraconazole-loaded solid dispersion without crystalline change with improved bioavailability, Arch Pharm. Res. (Seoul) (2010), https://doi.org/10.1007/s12272-010-0812-2.

[20] J.C. Dinunzio, J.R. Hughey, C. Brough, D.A. Miller, R.O. Williams, J.W. McGinity, Production of advanced solid dispersions for enhanced bioavailability of itraconazole using KinetiSol® Dispersing, Drug Dev. Ind. Pharm. (2010), https://doi.org/10.3109/03639041003652973.

[21] B. Hens, M. Bermejo, Y. Tsume, I. Gonzalez-Alvarez, H. Ruan, K. Matsui, G.E. Amidon, K.L. Cavanagh, G. Kuminek, G. Benninghoff, J. Fan, N. Rodríguez-Hornedo, G.L. Amidon, Evaluation and optimized selection of supersaturating drug delivery systems of posaconazole (BCS class 2b) in the gastrointestinal simulator (GIS): an in vitro-in silico-in vivo approach, Eur. J. Pharmaceut. Sci. 115 (2018) 258–269, https://doi.org/10.1016/j.ejps.2018.01.039.

[22] R. Laitinen, K. Löbmann, H. Grohganz, P. Priemel, C.J. Strachan, T. Rades, Supersaturating drug delivery systems: the potential of co-amorphous drug formulations, Int. J. Pharm. 532 (2017) 1–12, https://doi.org/10.1016/j.ijpharm.2017.08.123.

[23] E.J.A. Suys, D.K. Chalmers, C.W. Pouton, C.J.H. Porter, Polymeric precipitation inhibitors promote fenofibrate supersaturation and enhance drug absorption from a type IV lipid-based formulation, Mol. Pharm. 15 (2018) 2355–2371, https://doi.org/10.1021/acs.molpharmaceut.8b00206.

[24] J. Tang, H. Wei, H. Liu, H. Ji, D. Dong, D. Zhu, L. Wu, Pharmacokinetics and biodistribution of itraconazole in rats and mice following intravenous administration in a novel liposome formulation, Drug Deliv. 17 (2010) 223–230, https://doi.org/10.3109/10717541003667822.

[25] Y. Sun, M. Zhang, C. Liu, S. Zhou, W. Zhang, T. Wang, M. Zhou, X. Liu, Y. Wang, Y. Sun, J. Sun, Development of Liposome containing sodium deoxycholate to enhance oral bioavailability of itraconazole, Asian J. Pharm. Sci. (2017), https://doi.org/10.1016/j.ajps.2016.05.006.

[26] J. Wang, G. Huang, Preparation of itraconazole-loaded liposomes coated by carboxymethyl chitosan and its pharmacokinetics and tissue distribution, Drug Deliv. (2011), https://doi.org/10.3109/10717544.2011.621988.

[27] Y. Yi, H.J. Yoon, B.O. Kim, M. Shim, S.O. Kim, S.J. Hwang, M.H. Seo, A mixed polymeric micellar formulation of itraconazole: characteristics, toxicity and pharmacokinetics, J. Contr. Release (2007), https://doi.org/10.1016/j.jconrel.2006.10.001.

[28] W. Chen, B. Gu, H. Wang, J. Pan, W. Lu, H. Hou, Development and evaluation of novel itraconazole-loaded intravenous nanoparticles, Int. J. Pharm. (2008), https://doi.org/10.1016/j.ijpharm.2008.05.039.

[29] X. Ling, Z. Huang, J. Wang, J. Xie, M. Feng, Y. Chen, F. Abbas, J. Tu, J. Wu, C. Sun, Development of an itraconazole encapsulated polymeric nanoparticle platform for effective antifungal therapy, J. Mater. Chem. B (2016), https://doi.org/10.1039/c5tb02453f.

[30] X. Bian, S. Liang, J. John, C.H. Hsiao, X. Wei, D. Liang, H. Xie, Development of PLGA-based itraconazole injectable nanospheres for sustained release, Int. J. Nanomed. (2013), https://doi.org/10.2147/IJN.S54040.

[31] L. Qiu, B. Hu, H. Chen, S. Li, Y. Hu, Y. Zheng, X. Wu, Antifungal efficacy of itraconazole-loaded TPGS-b-(PCL-ran-PGA) nanoparticles, Int. J. Nanomed. (2015), https://doi.org/10.2147/IJN.S71616.

[32] C.J.H. Porter, N.L. Trevaskis, W.N. Charman, Lipids and lipid-based formulations: optimizing the oral delivery of lipophilic drugs, Nat. Rev. Drug Discov. 6 (2007) 231–248, https://doi.org/10.1038/nrd2197.

[33] A. Bernkop-Schnürch, A. Müllertz, T. Rades, Self-emulsifying drug delivery systems (SEDDS) – the splendid comeback of an old technology, Adv. Drug Deliv. Rev. (2019), https://doi.org/10.1016/j.addr.2019.08.002.

[34] Y.S. Rhee, C.W. Park, T.Y. Nam, Y.S. Shin, S.C. Chi, E.S. Park, Formulation of parenteral microemulsion containing itraconazole, Arch Pharm. Res. (Seoul) (2007), https://doi.org/10.1007/BF02977787.

[35] J.K. Kim, J.S. Park, C.K. Kim, Development of a binary lipid nanoparticles formulation of itraconazole for parenteral administration and controlled release, Int. J. Pharm. (2010), https://doi.org/10.1016/j.ijpharm.2009.09.008.

[36] J.Y. Hong, J.K. Kim, Y.K. Song, J.S. Park, C.K. Kim, A new self-emulsifying formulation of itraconazole with improved dissolution and oral absorption, J. Contr. Release 110 (2006) 332–338, https://doi.org/10.1016/j.jconrel.2005.10.002.

[37] C.A.S. Bergström, W.N. Charman, C.J.H. Porter, Computational prediction of formulation strategies for beyond-rule-of-5 compounds, Adv. Drug Deliv. Rev. (2016), https://doi.org/10.1016/j.addr.2016.02.005.

[38] H.D. Williams, Y. Sahbaz, L. Ford, T.H. Nguyen, P.J. Scammells, C.J.H. Porter, Ionic liquids provide unique opportunities for oral drug delivery: structure optimization and in vivo evidence of utility, Chem. Commun. (2014), https://doi.org/10.1039/c3cc48650h.

[39] Y. Sahbaz, H.D. Williams, T.H. Nguyen, J. Saunders, L. Ford, S.A. Charman, P.J. Scammells, C.J.H. Porter, Transformation of poorly water-soluble drugs into lipophilic ionic liquids enhances oral drug exposure from lipid based formulations, Mol. Pharm. (2015), https://doi.org/10.1021/mp500790t.

[40] H.D. Williams, L. Ford, A. Igonin, Z. Shan, P. Botti, M.M. Morgen, G. Hu, C.W. Pouton, P.J. Scammells, C.J.H. Porter, H. Benameur, Unlocking the full potential of lipid-based formulations using lipophilic salt/ionic liquid forms, Adv. Drug Deliv. Rev. 142 (2019) 75–90, https://doi.org/10.1016/j.addr.2019.05.008.

[41] H. Zhong, G. Chan, Y. Hu, H. Hu, D. Ouyang, A comprehensive map of FDA-approved pharmaceutical products, Pharmaceutics (2018), https://doi.org/10.3390/pharmaceutics10040263.

[42] R. Holm, Bridging the gaps between academic research and industrial product developments of lipid-based formulations, Adv. Drug Deliv. Rev. 142 (2019) 118–127, https://doi.org/10.1016/j.addr.2019.01.009.

[43] J. Rantanen, J. Khinast, The future of pharmaceutical manufacturing sciences, J. Pharmacol. Sci. (2015), https://doi.org/10.1002/jps.24594.

[44] A. Kumar, F. Chen, A. Mozhi, X. Zhang, Y. Zhao, X. Xue, Y. Hao, X. Zhang, P.C. Wang, X.J. Liang, Innovative pharmaceutical development based on unique properties of nanoscale delivery formulation, Nanoscale (2013), https://doi.org/10.1039/c3nr01525d.

[45] Z. Vinarov, V. Katev, D. Radeva, S. Tcholakova, N.D.D. Denkov, Micellar solubilization of poorly water-soluble drugs: effect of surfactant and solubilizate molecular structure, Drug Dev. Ind. Pharm. 44 (2018) 677–686, https://doi.org/10.1080/03639045.2017.1408642.

[46] Z. Vinarov, G. Gancheva, V. Katev, S.S. Tcholakova, Albendazole solution formulation via vesicle-to-micelle transition of phospholipid-surfactant aggregates, Drug Dev. Ind. Pharm. (2018), https://doi.org/10.1080/03639045.2018.1438461.

[47] Z. Vinarov, P. Dobreva, S. Tcholakova, Effect of surfactant molecular structure on Progesterone solubilization, J. Drug Deliv. Sci. Technol. (2018), https://doi.org/10.1016/j.jddst.2017.09.014.

[48] J.T.H. Ong, E. Manoukian, Micellar solubilization of timobesone acetate in aqueous and aqueous propylene glycol solutions of nonionic surfactants, Pharm. Res. An Off. J. Am. Assoc. Pharm. Sci. (1988), https://doi.org/10.1023/A:1015903827042.

[49] P.A. Bhat, A.A. Dar, G.M. Rather, Solubilization capabilities of some cationic, anionic, and nonionic surfactants toward the poorly water-soluble antibiotic drug erythromycin, J. Chem. Eng. Data (2008), https://doi.org/10.1021/je700659g.

[50] A.K. Krishna, D.R. Flanagan, Micellar solubilization of a new antimalarial drug, β-arteether, J. Pharmacol. Sci. 78 (1989) 574–576, https://doi.org/10.1002/jps.2600780713.

[51] K.A. Alkhamis, H. Allaboun, W.Y. Al-Momani, Study of the solubilization of gliclazide by aqueous micellar solutions, J. Pharmacol. Sci. (2003), https://doi.org/10.1002/jps.10350.

[52] B.W. Barry, D.I.D.E. Eini, Solubilization of hydrocortisone, dexamethasone,

testosterone and progesterone by long-chain polyoxyethylene surfactants, J. Pharm. Pharmacol. (1976), https://doi.org/10.1111/j.2042-7158.1976.tb04133.x.
[53] C. de O. Rangel-Yagui, A. Pessoa, L.C. Tavares, Micellar solubilization of drugs, J. Pharm. Pharmaceut. Sci. (2005).
[54] FDA/Center for DrugEvaluation and Research, FDA inactive ingredients database, n.d. https://www.accessdata.fda.gov/scripts/cder/iig/ accessed January 25, 2020.
[55] E. Inkmann, U. Holzgrabe, 1H and 13C nuclear magnetic resonance studies of the sites of protonation in itraconazole and fluconazole, J. Pharmaceut. Biomed. Anal. 20 (1999) 297–307, https://doi.org/10.1016/S0731-7085(99)00042-4.
[56] Y. Shi, W. Porter, T. Merdan, L.C. Li, Recent advances in intravenous delivery of poorly water-soluble compounds, Expet Opin. Drug Deliv. (2009), https://doi.org/10.1517/17425240903307423.
[57] J. Van Den Abeele, M. Rayyan, I. Hoffman, E. Van de Vijver, W. Zhu, P. Augustijns, Gastric fluid composition in a paediatric population: age-dependent changes relevant for gastrointestinal drug disposition, Eur. J. Pharmaceut. Sci. 123 (2018) 301–311, https://doi.org/10.1016/j.ejps.2018.07.022.
[58] D. Riethorst, R. Mols, G. Duchateau, J. Tack, J. Brouwers, P. Augustijns, Characterization of human duodenal fluids in fasted and fed state conditions, J. Pharmacol. Sci. 105 (2016) 673–681, https://doi.org/10.1002/jps.24603.
[59] J.K. Guillory, P. Heinrich Stahl, Camile G. Wermuth, Handbook of Pharmaceutical Salts: Properties, Selection, and Use Edited, VHCA, Verlag Helvetica Chimica Acta, Zürich, Switzerland, and Wiley-VCH, Weinheim, Germany, 2002, https://doi.org/10.1021/jm030019n vix + 374 pp. 17.5 × 24.5 cm. ISBN 3-906, J. Med. Chem. (2003).
[60] B.C. Stephenson, C.O. Rangel-Yagui, A. Pessoa, L.C. Tavares, K. Beers, D. Blankschtein, Experimental and theoretical investigation of the micellar-assisted solubilization of ibuprofen in aqueous media, Langmuir (2006), https://doi.org/10.1021/la052530k.
[61] K. Stoyanova, Z. Vinarov, S. Tcholakova, Improving Ibuprofen solubility by surfactant-facilitated self-assembly into mixed micelles, J. Drug Deliv. Sci. Technol. 36 (2016) 208–215 https://www.sciencedirect.com/science/article/pii/S1773224716304713 accessed August 7, 2018.
[62] U. Thapa, K. Ismail, Urea effect on aggregation and adsorption of sodium dioctylsulfosuccinate in water, J. Colloid Interface Sci. (2013), https://doi.org/10.1016/j.jcis.2013.06.009.
[63] M.J. Rosen, J.T. Kunjappu, Surfactants and Interfacial Phenomena, fourth ed., (2012), https://doi.org/10.1002/9781118228920.
[64] S.E. Anachkov, K.D. Danov, E.S. Basheva, P.A. Kralchevsky, K.P. Ananthapadmanabhan, Determination of the aggregation number and charge of ionic surfactant micelles from the stepwise thinning of foam films, Adv. Colloid Interface Sci. (2012), https://doi.org/10.1016/j.cis.2012.08.003.
[65] N. Patra, A. Mal, A. Dey, S. Ghosh, Influence of solvent, electrolytes, β-CD, OTAB on the krafft temperature and aggregation of sodium tetradecyl sulfate, J. Mol. Liq. (2019), https://doi.org/10.1016/j.molliq.2019.02.002.
[66] M. Maswal, O.A. Chat, S. Jabeen, U. Ashraf, R. Masrat, R.A. Shah, A.A. Dar, Solubilization and co-solubilization of carbamazepine and nifedipine in mixed micellar systems: insights from surface tension, electronic absorption, fluorescence and HPLC measurements, RSC Adv. (2015), https://doi.org/10.1039/c4ra09870f.
[67] P.J. Tummino, A. Gafni, Determination of the aggregation number of detergent micelles using steady-state fluorescence quenching, Biophys. J. (1993), https://doi.org/10.1016/S0006-3495(93)81528-5.
[68] Y. Fan, Y. Li, G. Yuan, Y. Wang, J. Wang, C.C. Han, H. Yan, Z. Li, R.K. Thomas, Comparative studies on the micellization of sodium bis(4-phenylbutyl) sulfosuccinate and sodium bis(2-ethylhexyl) sulfosuccinate and their interaction with hydrophobically modified poly(acrylamide), Langmuir (2005), https://doi.org/10.1021/la047129x.
[69] B. Tah, P. Pal, S. Mishra, G.B. Talapatra, Interaction of insulin with anionic phospholipid (DPPG) vesicles, Phys. Chem. Chem. Phys. (2014), https://doi.org/10.1039/c4cp03028a.
[70] D.W.R. Gruen, E.H.B. de Lacey, The packing of amphiphile chains in micelles and bilayers, in: K.L. Mittal, B. Lindman (Eds.), Surfactants Solut. Springer, Boston, MA, 1984, pp. 279–306.
[71] J.N. Israelachvili, Intermolecular and Surface Forces, third ed., (2011), https://doi.org/10.1016/C2011-0-05119-0.